Advanced Ceramics Progress: Vol. 8, No. 2, (Spring 2022) 61-72

Materials and Energy Research Center
MERC

Contents lists available at ACERP

Advanced Ceramics Progress

Journal Homepage: www.acerp.ir

Original Research Article

Improvement of the Effective Parameters of 1-3 Piezocomposite Using Multi-Layer Polymer and PMN-PT Relaxor Single Crystal

Bentolhoda Amanat [a, *]

[a] *Assistant Professor, Department of Physics, Faculty of Sciences, Payame Noor University, Tehran, Tehran, Iran*

* Corresponding Author Email: amanat@pnu.ac.ir (B. Amanat)

URL: https://www.acerp.ir/article_159842.html

ARTICLE INFO

Article History:

Received 13 August 2022
Received in revised form 20 September 2022
Accepted 24 September 2022

Keywords:

1-3 Piezocomposite
Multi-Layer Polymer
Filling Fraction
Effective Parameter
PMN-PT

ABSTRACT

In this study, 1-3 piezocomposite with multi-layer polymer based on PZT piezoceramics and PMN-0.33PT relaxor single crystal was modeled and analyzed, and the obtained results were assessed. Recently, PMN-PT relaxor single crystals have been introduced as a suitable alternative to the PZTs due to their great piezoelectric coefficients. In addition, use of multi-layer polymers made from a combination of a polymer with a high stiffness coefficient for maintaining strength and a polymer with a much lower stiffness coefficient for increasing the electromechanical coupling coefficient improved the parameters of 1-3 piezocomposite. In addition, 1-3 piezocomposite with a multi-layer polymer based on PMT-PT increased the electromechanical coupling coefficient as well as the bandwidth of the filling fraction with the maximum value of k_t. This finding facilitated producing a piezocomposite at low filling fractions with very high k_t and very low characteristic acoustic impedance close to the characteristic impedance of the environment. It was shown that in the case where 75 % of the volume of the polymer phase was composed of silicone rubber, 1-3 piezocomposite with multi-layer polymer based on PMN-0.33PT single crystal could increase the electromechanical coupling coefficient to values greater than 0.95. In addition, in this case, it is possible to achieve a coupling coefficient of 0.94 and a characteristic impedance of 7 MRayl at the filling fraction of 0.2. The obtained results were analytically confirmed through the finite element numerical results.

https://doi.org/10.30501/acp.2022.355196.1099

1. INTRODUCTION

Piezoelectric materials are widely used in engineering sciences, materials, and smart structures [1,2]. The piezoelectric effect was first discovered by the Curie brothers in quartz [3,4]. A year later, in 1881, the converse piezoelectric effect was discovered by Lippmann [5]. Then, Newnham proposed the idea of polymer composites known as piezocomposite based on the PZT ceramics in 1978. Piezocomposite usually consists of two phases. The first phase is the active or piezoelectric phase while second phase is the inactive or the polymer phase with a specific connection mode, mass or volume ratio, and spatial geometric distribution [6]. In composites with two phases, 10 compounds are identified by two numbers [7].

One of the most widely used piezocomposites is 1-3 piezocomposite. High-performance 1-3 piezocomposites are widely utilized in high-frequency ultrasound transducers that are used for medical imaging [8-11]. Generally, 1-3 piezocomposite is preferred to the standard piezoceramics owing to its advantageous

Please cite this article as: Amanat, B., "Improvement of the Effective Parameters of 1-3 Piezocomposite Using Multi-Layer Polymer and PMN-PT Relaxor Single Crystal", ***Advanced Ceramics Progress***, Vol. 8, No. 2, (2022), 61-72. https://doi.org/10.30501/acp.2022.355196.1099

characteristics namely its low acoustic impedances, high electromechanical coupling coefficients, and high bandwidth [12-14]. However, compared to the bulk piezoceramics, piezocomposites components have some drawbacks such as their relatively high costs and limited operating temperature range [15,16]. The mentioned piezocomposite is commonly applied in Non-Destructive Testing (NDT) and sonar systems [17]. Yet, the biggest market for such materials is the medical diagnostic ultrasound market. Current medical ultrasound imaging systems cannot efficiently operate without application of 1-3 piezocomposite [18].

Owing to their beneficial features, they have been popular subjects of many research studies conducted to further improve the determining parameters in two ways: first, using materials with better piezoelectric properties in the piezocomposite structure and second, making changes in the structure and composition of the piezocomposite to facilitate the improvement of the electromechanical coupling coefficient parameters as much as possible so that the characteristic acoustic impedance (Z) of the piezocomposite would be close to the characteristic acoustic impedance of water (Z_{water} = 1.5 MRayl).

PZT ceramic is characterized by high electromechanical properties and advantages such as low cost and ease of production [19]. However, to overcome the problems caused by application of this material, a great deal of research has been conducted on how to replace the PZTs with more efficient materials with much better performance. In recent years, a new class of single-crystal piezoelectric materials called relaxor-based ferroelectric single crystals has received considerable attention mainly because these crystals, such as relaxor ferroelectric PMN-PT single crystals, have much higher and better piezoelectric properties than other ones such as quartz and piezoceramic materials (PZTs). Owing to their very high dielectric and piezoelectric constants, they have a very good electromechanical coupling coefficient, compared to the PZT piezoceramics. It is expected that 1-3 piezocomposites based on PMN-PT single crystal would have much better piezoelectric properties than those of their counterparts [18].

Efforts have been made to improve the electromechanical coupling coefficient by changing the structure of piezocomposites. In this regard, several researchers prepared a 1-3 piezocomposite by using other flexible polymers and attempted to enhance its electromechanical coupling coefficient [20,21]. According to the observations, the more flexible the polymer was, the more it succeeded in enhancing the electromechanical coupling of the composite [22]. However, high flexibility makes the composite susceptible to deformation [23,24]. A recent suitable solution to this problem is to use multi-layer piezocomposites.

Therefore, to increase the electromechanical coupling coefficient and decrease the characteristic acoustic impedance of 1-3 piezocomposite, the current study suggested application of relaxor ferroelectric PMN-0.33PT single crystals in a piezocomposite with a three-layer polymer structure. It is expected that using this relaxor single crystal in the structure of a 1-3 piezocomposite with a three-layer polymer will yield the desired results.

Different models have been designed to examine the effective properties of piezocomposites [25]. In this paper, some series and parallel theoretical models were used to determine the effective properties of three-layer piezocomposite [26,27]. Based on the results from the theoretical model and finite element numerical method, the behavior of electromechanical coupling coefficient and characteristic acoustic impedance of 1-3 piezocomposite were evaluated, and the obtained results were compared with each other. As observed, 1-3 piezocomposite with a three-layer polymer based on PMN-PT is characterized by a much better electromechanical coupling coefficient and acoustic impedance than the conventional 1-3 piezocomposites.

2. THEORETICAL FOUNDATIONS

1-3 Piezocomposite with a multi-layer polymer structure includes piezoceramic rods that are placed in a multi-layer polymer (one layer of polyethylene in the middle and two layers of silicone rubber at the top and bottom of piezocomposite). Figure 1 illustrates the structure of 1-3 piezocomposite with multi-layer polymer. In this model, the thickness direction of the piezocomposite is assumed to be in the z axis, and its transverse directions are assumed to be along the x and y axes. Piezoceramic columns are placed along the direction of the thickness of the piezocomposite. In the following, the relationships that clarify a piezoelectric material are presented [28].

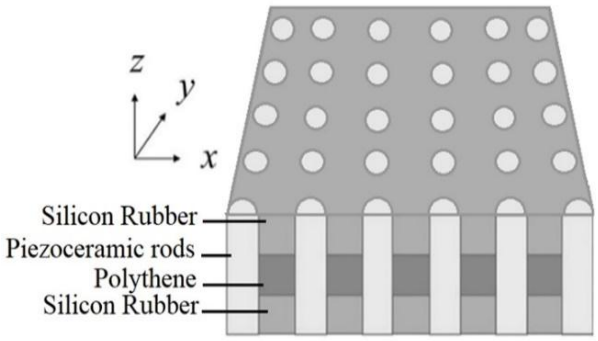

Figure 1. Schematic of 1-3 piezocomposite with three-layer polymer

$$\begin{cases} T_i = c_{ij}^D S_j + h_{ni} D_n \\ E_m = -h_{mj} S_j + \beta_{mn}^S D_n \end{cases} \quad (1)$$

where T is the mechanical stress tensor, S the mechanical strain tensor, D the electric charge displacement vector, E the electric field vector, c^D the elastic stiffness tensor in constant electric displacement, h the piezoelectric coefficient, and β^S the imprimitivity tensor in constant strain [29]. The polarization axis of the piezoelectric material is considered to be in the z axis. Of note, 1-3 piezocomposite can be considered as a homogeneous piezoelectric material with new effective parameters [30].

A series of assumptions based on uniform field theories as well as the rule of mixtures was taken into consideration to obtain the effective material parameters [31]. In the thickness mode, the lateral dimensions of the composite are sufficiently larger than the thickness one. According to the properties of the thickness mode, the piezocomposite was assumed to be parallel and symmetrical in the x and y axes, respectively.

Since it is quite difficult to obtain the relationship describing a piezocomposite using full field equations. Therefore, some simplifying approximations were used to obtain the essential physics. Given that the piezocomposite layers are in series on top of each other, due to the homogeneous displacement of the layers, the normal strains in the transverse directions of the piezocomposite are considered the same and equal to the effective strain for all three layers. In this regard, we assume that the strain and electric field in all piezocomposite plates that are placed on top of each other independent of x and y axes.

Therefore, shear strains and electric fields in the x and y axes can be ignored. In addition, the amount of electrical displacement of each layer and effective electrical displacement in transverse directions will be equal to zero. Since the polymers are connected in series, the vertical effective strain (S_3) of 1-3 piezocomposite with three-layer polymer along the thickness direction is equal to the weighted sum of the strains of all layers.

Moreover, the effective stress along the thickness direction in the piezocomposite is equal to the stress value along the thickness direction in each layer. The transverse effective stresses (T_1, T_2) will also be equal to the weighted sum of the transverse stresses of each layer.

The electrode surfaces are perpendicular to the z axis. Therefore, the effective electric field in the z direction, which is the same direction as the thickness one, is equal to the sum of the electric field in each layer of the piezocomposite with three layers of polymer. Due to the perpendicularity of the electrode surfaces to the z axis, the electric displacement in each layer of piezocomposite is the same and equal to the effective electric displacement of the piezocomposite along the thickness direction [32].

According to the mentioned assumptions, the relationships between the effective the electric field E_3, stresses T_1 and T_3 for each layer can be obtained as [33,34]:

$$\bar{S}_3 = -2\frac{\bar{c}_{13}^D}{\bar{c}_{33}^D}\bar{S}_1 + \frac{1}{\bar{c}_{33}^D}\bar{T}_3 + \frac{\bar{h}_{33}}{\bar{c}_{33}^D}\bar{D}_3 \quad (2)$$

$$\bar{T}_1 = \left(\bar{c}_{11}^D + \bar{c}_{12}^D - 2\frac{(\bar{c}_{13}^D)^2}{\bar{c}_{33}^D}\right)\bar{S}_1 + \frac{\bar{c}_{13}^D}{\bar{c}_{33}^D}\bar{T}_3 + \left(\bar{c}_{13}^D\frac{\bar{h}_{33}}{\bar{c}_{33}^D} - \bar{h}_{31}\right)\bar{D}_3 \quad (3)$$

$$\bar{E}_3 = (2\bar{h}_{33}\frac{\bar{c}_{13}^D}{\bar{c}_{33}^D} - 2\bar{h}_{31})\bar{S}_1 + \frac{-\bar{h}_{33}}{\bar{c}_{33}^D}\bar{T}_3 + \left(\bar{\beta}_{33}^s - \frac{(\bar{h}_{33})^2}{\bar{c}_{33}^D}\right)\bar{D}_3 \quad (4)$$

The sign ($\bar{}$) above each parameter indicates the effective value of that parameter in a layer. In addition, for the effective strain, effective stress, and effective electric field, we have [34]:

$$\bar{\bar{S}}_3 = v_1\bar{S}_3^1 + v_2\bar{S}_3^2 + v_3\bar{S}_3^3 \quad (5)$$

$$\bar{\bar{T}}_1 = v_1\bar{T}_1^1 + v_2\bar{T}_1^2 + v_3\bar{T}_1^3 \quad (6)$$

$$\bar{\bar{E}}_3 = v_1\bar{E}_3^1 + v_2\bar{E}_3^2 + v_3\bar{E}_3^3 \quad (7)$$

The sign ($\bar{\bar{}}$) above T, E, and S parameters indicates their effective value in 1-3 piezocomposite with a three-layer polymer. In addition, v_1, v_2, and v_3 are the volume fraction of the first, second, and third layers, respectively. Equations (2), (3), and (4) are substituted in Equations (5), (6), and (7) and then simplified.

According to the relationships related to the thickness mode in piezoelectric materials, the final relationships for 1-3 piezocomposite with three-layer polymer in thickness mode will be as follows [28]:

$$\begin{cases} \bar{\bar{T}}_3 = \bar{\bar{c}}_{33}^D\bar{\bar{S}}_3 - \bar{\bar{h}}_{33}\bar{\bar{D}}_3 \\ \bar{\bar{E}}_3 = -\bar{\bar{h}}_{33}\bar{\bar{S}}_3 + \bar{\bar{\beta}}_{33}^S\bar{\bar{D}}_3 \end{cases} \quad (8)$$

where both $\bar{\bar{c}}_{33}^D$, $\bar{\bar{h}}_{33}$ and $\bar{\bar{\beta}}_{33}^S$ are obtained according to the coefficients of the piezocomposite components.

For the thickness mode, the electromechanical coupling coefficient (k_t), characteristic acoustic impedance, and the longitudinal velocity are obtained in the following equations [28]:

$$k_t = \sqrt{\frac{\bar{\bar{h}}_{33}^2}{\bar{\bar{c}}_{33}^D}\bar{\bar{\epsilon}}_{33}^S} \quad (9)$$

$$c_t^D = \sqrt{\frac{\bar{\bar{c}}_{33}^D}{\bar{\bar{\rho}}}} \quad (10)$$

$$Z = \bar{\bar{\rho}}.\overline{\overline{c_t^D}} \quad (11)$$

where $(\bar{\bar{\rho}})$ is the effective density which is defined as:

$$\bar{\bar{\rho}} = v_c\rho_c + (1 - v_c)(v_e\rho_e + (1 - v_e)\rho_s) \quad (12)$$

In the above relationship, v_c is the volume fraction of piezoceramic in the 1-3 piezocomposite, and v_e the volume fraction of epoxy resin in the inactive or polymer phase of the piezocomposite. In addition, ρ_c, ρ_e, and ρ_s represent the density of the active phase of piezocomposite, density of epoxy resin, and density of silicone rubber, respectively.

3. SOLUTION METHOD AND HYPOTHESES

Here, consider a piezocomposite 1-3 consisting of three polymer layers, as shown in Figure 1. Table 1 lists the characteristics of the constituent polymer layers. In this research, PZT-4, PZT-8, and PMN-PT piezoceramics were used as the active piezoelectric phase, and their specifications are given in Table 2.

We define the V_{SR} parameter as:

$$V_{SR}\% = \frac{\text{Silicon Rubber volume} \times 100}{\text{Silicon Rubber volume} + \text{Polythene volume}}$$

As a result, the filling fraction of piezoelectric phase in piezocomposite as defined as:

$$\text{filling fraction of piezoelectric phase} = \frac{\text{volume of piezoelectric phase material}}{\text{volume of piezocomposite}}$$

Based on Equations (9), (10), and (11), the electromechanical coupling coefficient, longitudinal velocity, and characteristic impedance, respectively, were plotted for different V_{SR} (V_{SR} =0 %, 25 %, 50 %, and 75 %) as the functions of active piezoelectric phase filling fraction.

In these figures, the horizontal axis shows the filling fraction of the active piezoelectric phase, and the plot corresponding to V_{SR} =0 (shown by the solid line in all plots) refers to the simple 1-3 piezocomposite with monolayer polymer.

To confirm the results, the electromechanical coupling coefficient and characteristic acoustic impedance at several filling fractions (0.01, 0.1, 0.2, 0.3, 0.4, 0.5, 0.6, 0.7, and 0.8) for V_{SR} = 50 % were calculated using the finite element numerical method. Then, the numerical results were compared with the theoretical results. For this purpose, first, the piezocomposite electrical impedance was extracted as a function of frequency for the mentioned states.

TABLE 1. Specifications of polymers

Material parameters of the polymer		
Parameter	Polythene	Silicon Rubber
ρ (kg/)	1180	1150
c_{11}^E (GPa)	5.54	0.004
c_{12}^E (GPa)	2.98	0.0023
$\varepsilon_{11}^S(10^{-10})$	0.204	3.45

TABLE 2. Specifications of piezoceramics

Material parameters of the piezoelectric			
Parameter	PZT-8	PZT-4	PMN-0.33PT
ρ	7600	7500	8038
c_{11}^E (GPa)	149	139	115
c_{12}^E (GPa)	81.1	77.8	103
c_{13}^E (GPa)	81.1	74.3	102
c_{33}^E (GPa)	132	115	103.8
e_{31} (c/m^2)	-4.1	-5.2	-3.390
e_{33} (c/m^2)	14	15.1	20.4
$\varepsilon_{11}^S/\varepsilon_0$	900	730	1434
$\varepsilon_{33}^S/\varepsilon_0$	600	635	679

Figure 2 shows a schematic view of the electrical impedance curve as a function of frequency.

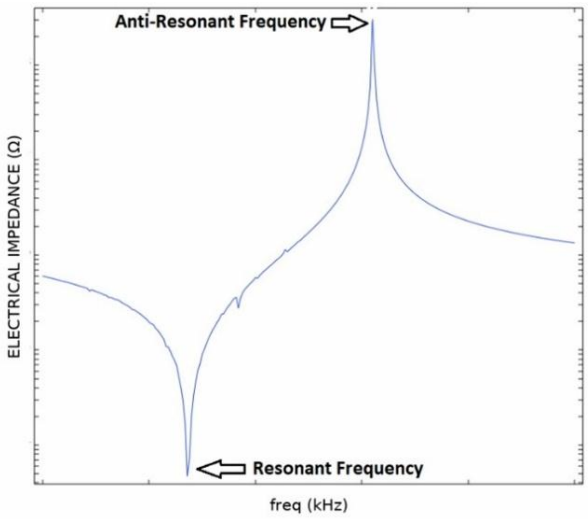

Figure 2. The electrical impedance of a piezoelectric material as a function of frequency

Based on this curve, the resonance and anti-resonance frequencies as well as the characteristic impedance and the electromechanical coupling coefficient were extracted through Equations (13) and (14) [34].

$$k_t = \sqrt{\frac{\pi f_s}{2f_p}\tan\frac{\pi(f_p - f_s)}{2f_p}} \quad (13)$$

$$Z = 2\bar{\rho}f_p t \quad (14)$$

where f_p is the anti-resonance frequency, f_s the resonance frequency, and t the thickness of the piezocomposite.

In practice, a network analyzer was employed to extract the electrical impedance diagram in terms of frequency. In addition, Relations (13) and (14) are used to calculate the electromechanical coupling coefficient and characteristic acoustic impedance.

3. RESULTS AND DISCUSSION

Figure 3 illustrates the variations of the electromechanical coupling coefficient for a 1-3 piezocomposite with a three-layer polymer based on PZT-8 piezoceramic at V_{SR} = 0 %, 25 %, 50 %, and 75 %. As observed in all four cases, V_{SR}, with an increase in the piezoelectric phase filling fraction from 0.1 to 0.3, the electromechanical coupling coefficient would rapidly increase. However, its value remains almost constant in a certain range (0.3 to 0.7) which is near to the maximum value of the electromechanical coupling coefficient. Next, with an increase in the filling fraction from 0.7 to 0.9, the coupling coefficient would rapidly decrease. The first point in this diagram is that upon increasing the value of V_{RS}, the value of k_t would consequently increase. As a result, the maximum value of k_t increases from 0.625 at V_{SR} =0 % to about 0.638 at V_{SR} =75 %, indicating an increase of 2 % in the maximum k_t value. Such an increase in the coupling coefficient results from using silicone rubber polymer, which is more flexible than polyethylene, as part of the inactive phase in the piezocomposite. The effective factor in this problem is the values of the elastic constant c_{11} in the polymer. The lower the value of this constant, the higher the electromechanical coupling coefficient.

According to the observations, with an increase in the V_{SR}, the electromechanical coupling coefficient reaches its maximum value in a larger range of the piezoceramic filling fraction; therefore, in the case of V_{SR}=0 %, the electromechanical coupling coefficient in the piezoceramic filling fraction range of 0.45 to 0.65 of the reaches its maximum value. In the case of V_{SR} =75 %, this range is from about 0.3 to 0.8, meaning that this range increased almost 2.5 times. Increasing the width of the filling fraction with the maximum k_t allows for more

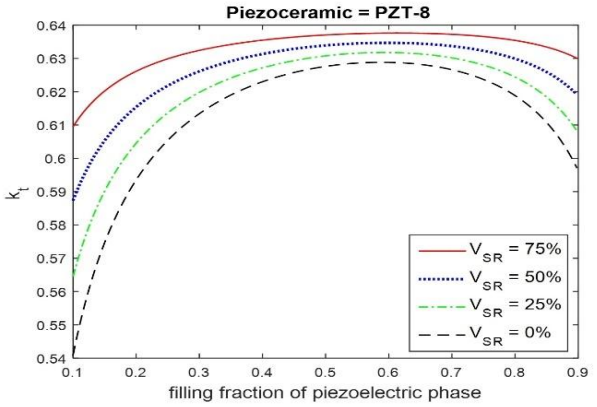

Figure 3. Variations in the electromechanical coupling factor for 1-3 piezocomposite with multi-layer polymer versus variations in the filling fraction of piezoceramic PZT-8 for different values of V_{SR}

freedom in determining other parameters such as the characteristic acoustic impedance. In fact, at V_{SR} =75 %, values near the maximum value of k_t are obtained in a larger range of filling fraction versus V_{SR} = 0 %.

In addition, at the filling fraction of 0.1 in V_{SR} =0 %, the value of k_t equals 0.54 while in V_{SR}=75 %, it equals 0.61. In other words, at the filling fraction of 0.1, the k_t value was improved up to about 13 %. Similarly, at the filling fractions of 0.9 and 0.5, there was about 5.5 % and 3 % increase in k_t, respectively.

Figure 4 shows the variations of the electromechanical coupling coefficient with the same conditions as before for 1-3 piezocomposite with a three-layer polymer based on piezoceramic PZT-4. Here, like the previous case, the electromechanical coupling coefficient increased with an increase in the value of V_{SR} at a constant filling fraction.

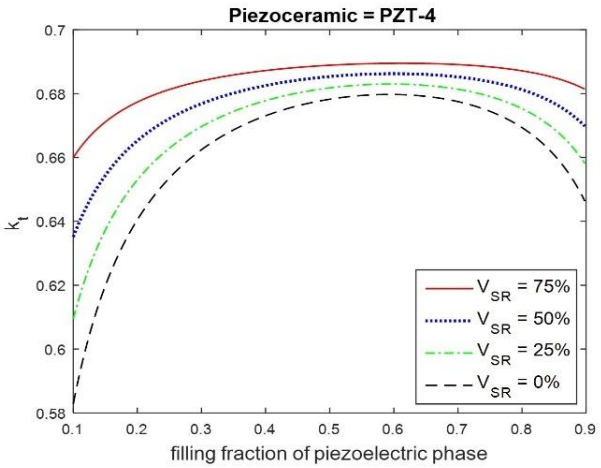

Figure 4. Variations in the electromechanical coupling factor for 1-3 piezocomposite with multi-layer polymer versus variations in the filling fraction of piezoceramic PZT-4 for different values of V_{SR}

Therefore, its maximum value of k_t from about 0.675 at V_{SR} =0 % increases up to about 0.69 at V_{SR}=75 %. That is, the k_t value increased up to about 2.2 % which a change in the V_{SR} from 0 % to 75 % at the filling fraction of 0.5. Such an increase in the k_t value by variation V_{SR} at the filling fractions 0.1 and 0.9 is about 14 % and 5 %, respectively.

Further, the bandwidth of the filling fraction where the value of k_t is constant at its maximum value considerably increased at V_{SR}=75 %, compared to that at V_{SR}=0 %.

Upon using PZT-4, the maximum value of k_t at the filling fraction of 0.5 and V_{SR}=75 % is equal to 0.688. This value shows an increase of about 8 % compared to that in the previous case where PZT-8 was used as the active phase. Such an increase occurs as a result of the higher value of k_t in PZT-4 than that of PZT-8.

Figure 5 shows the variations in the electromechanical coupling coefficient for 1-3 piezocomposite with a three-layer polymer based on PMN-0.33PT single crystal under the same conditions as before. In this figure, similar to Figures 3 and 4, the value of the coupling coefficient increases with an increase in the V_{SR} value from 0 % to 75 % at the constant filling fraction. The percentages of such increase at the volume fractions of about 0.5, 0.1, and 0.9 were 1.1 %, 16 %, and 8 %, respectively. This value is higher than that in the case where PZT-4 and PZT-8 were used as an active phase in the piezocomposite. On the contrary, the maximum value of k_t in this case was obtained as 0.95 at the filling fraction of 0.5 and V_{SR}=75 %, indicating a 38 % increase compared to the case where PZT-4 was used as the active phase. Such an increase in the maximum value of k_t results from the high electromechanical coupling coefficient of PMN-0.33PT single crystal. Apparently, use of PMN-0.33PT single crystal could significantly improve the electromechanical coupling coefficient.

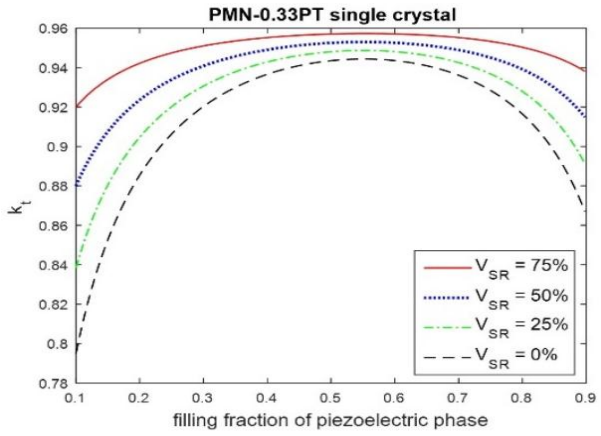

Figure 5. Variations in the electromechanical coupling factor for 1-3 piezocomposite with multi-layer polymer versus changes in the filling fraction of PMN-033PT single crystal for different values of V_{SR}

In the followingis examined the longitudinal velocity changes as a function of active phase filling fractions for 1-3 piezocomposite with a three-layer polymer for V_{SR} = 0 %, 25 %, 50 %, and 75 %.

Figure 6 shows the longitudinal velocity changes for 1-3 piezocomposite with three-layer polymer based on PZT-8. According to Figure 6, in general, the longitudinal velocity at V_{SR}=0 %, 25 %, 50 %, and 75 % starts to decrease with a slow slope as the filling fraction decreases by below 0.9. This trend continues until the filling fraction of 0.4 is reached; however, at the volume fraction values lower than 0.4, the decrease in the longitudinal velocity continues at higher rates. The effect of changing V_{SR} from 0 % to 75 % on the reduction of longitudinal velocity is much greater in the filling fractions close to 0.1 and 0.9. In this regard, at the filling fraction of 0.1 and V_{SR}=75 %, the longitudinal velocity is equal to 2800 m/s, showing a reduction of about 250 m/s compared to that in the case of V_{SR}=0 %. At the filling fraction of 0.9, the amount of such decrease is about 100 m/s. However, in the filling fraction range of 0.5 to 0.7, the longitudinal velocity does not change with variations in the V_{SR}, and these variations depend only on the changes in the piezoelectric active phase filling fraction.

Figure 7 shows the longitudinal velocity changes in 1-3 piezocomposite with a three-layer polymer based on PZT-4 as the function of piezoceramic filling fraction. The behavior of the longitudinal velocity changes in Figure 7 is similar to the changes in Figure 6. At the filling fractions of 0.1 and 0.9, the change in V_{SR} would cause a decrease in the longitudinal velocity by 220 m/s and 70 m/s, respectively, and in the filling fraction range of about 0.4 to 0.8, changes in V_{SR} do not have much effect on the longitudinal velocity. These changes result from the variations in the piezoceramic filling fraction.

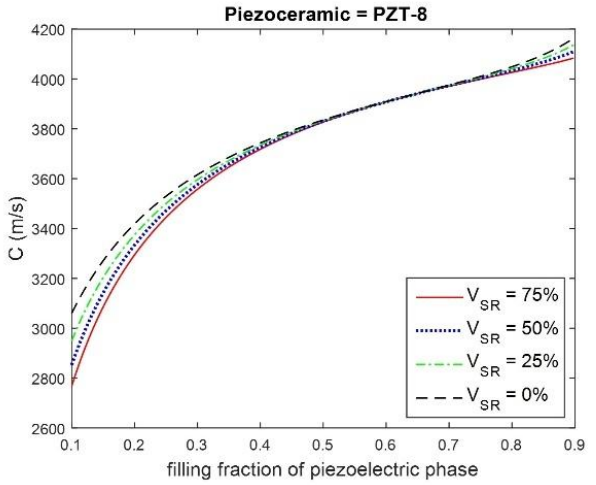

Figure 6. Variation of Longitudinal velocity for 1-3 piezocomposite with multi-layer polymer versus to changes in filling fraction of piezoceramic PZT-8 for different values of V_{SR}

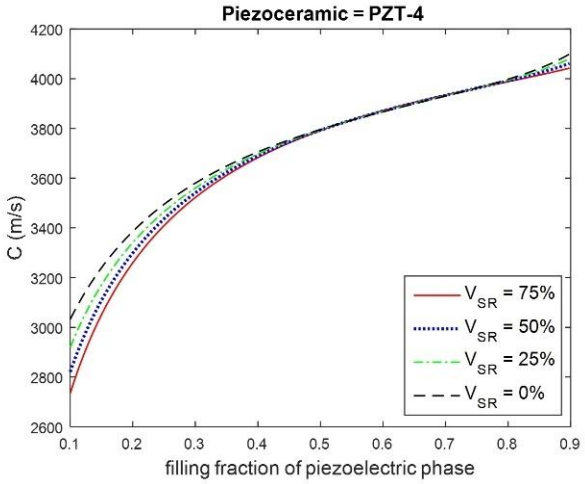

Figure 7. Variation of Longitudinal velocity for 1-3 piezocomposite with multi-layer polymer versus to changes in filling fraction of piezoceramic PZT-4 for different values of V_{SR}

As observed in Figures 6 and 7, at different volume fractions, the longitudinal velocity at V_{SR}=0 % is higher than those at V_{SR} = 25 %, 50 %, and 75 %. Yet, at the filling fraction of approximately 0.6, the longitudinal velocity at V_{SR}=0 % is slightly lower than those at other values of V_{SR}.

Figure 8 represents the longitudinal velocity changes in 1-3 piezocomposite with a three-layer polymer based on PMN-0.33PT as a function of filling fraction. The general behavior of this diagram is similar to those shown in Figures 6 and 7. With a reduction in the volume fraction value, the longitudinal velocity first decreases and then in the range of filling fractions of 0.6 to 0.4, it slightly decreases. In addition, at the volume fraction of 0.4, the longitudinal velocity begins to decrease with a relatively large slope.

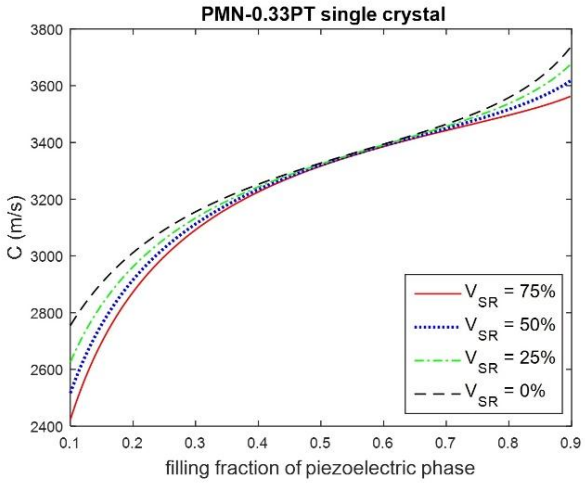

Figure 8. Variation of Longitudinal velocity for 1-3 piezocomposite with multi-layer polymer versus to changes in filling fraction of piezoceramic PMN-0.33PT for different values of V_{SR}

At the filling fraction of 0.1, the longitudinal velocity decreases from about 2750 m/s at V_{SR}=0 % to 2450 m/s at V_{SR}=75 %. At the filling fraction of 0.9, with a change in the value of V_{SR}, the longitudinal velocity decreases from about 3750 m/s at V_{SR}=0 % to 3550 m/s at V_{SR}=75 %. Therefore, the amount of longitudinal velocity changes in the filling fractions 0.1 and 0.9 are equal to 300m/s and 200m/s, respectively. In addition, as shown in Figure 8, in the volume fraction range of 0.6 to 0.5, the longitudinal velocity remains almost constant with a change in the V_{SR}; hence, the variations in the longitudinal velocity depend only on the variations in the filling fraction of the PMN-0.33PT. A comparison of Figures 6, 7, and 8 shows that compared to the case while PZT-4 and PZT-8 are applied, when PMN-0.33PT is used in the 1-3 piezocomposite with three-layer polymer, a reduction of at least 10 % is observed in the longitudinal velocity.

In the following, the changes in the characteristic acoustic impedance in 1-3 piezocomposite with multi-layer polymer is assessed based on piezoceramics PZT-4 and PZT-8 and PMN-0.33PT single crystal. Figure 9 shows the changes in the characteristic acoustic impedance of 1-3 piezocomposite with three-layer polymer based on piezoceramic PZT-8.

As observed in Figure 9, upon decreasing the piezoceramic filling fraction from 0.9 to 0.1, the characteristic acoustic impedance would also decrease, following an almost constant slope from about 28 MRayl to about 5 MRayl. This reduction is caused by a reduction in the piezoceramic filling fraction and effective density of the piezocomposite, as shown in Equation (12). In addition, increasing the amount of polymer by reducing the piezoceramic filling fraction also makes the

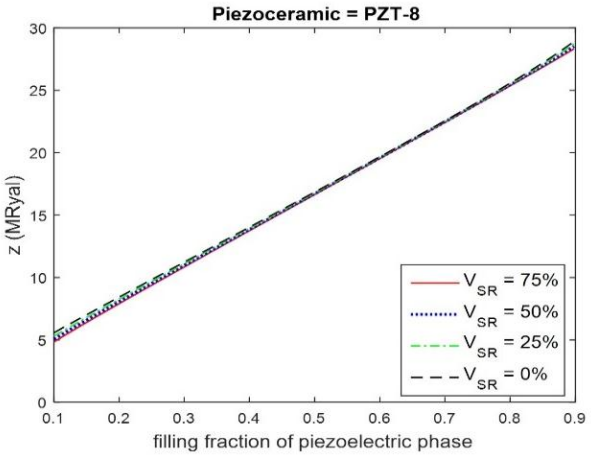

Figure 9. Variation of characteristic impedance for 1-3 piezocomposite with multi-layer polymer versus changes in the filling fraction of piezoceramic PZT-8 for different values of V_{SR}

piezocomposite softer than usual. As the V_{SR} value changed from 0 % to 75 %, a negligible decrease was observed in the characteristic impedance at a constant filling fraction, which was also caused by an increase in the proportion of silicone rubber.

Figure 10 depicts the diagram of the characteristic impedance changes for 1-3 piezocomposite with a three-layer polymer based on piezoceramic PZT-4. This diagram also exhibits a behavior similar to that observed in Figure 9. Upon decreasing the filling fraction in the range of 0.9 to 0.1, the characteristic acoustic impedance would also decrease almost linearly. Further, with a change in the V_{SR}, the value of the characteristic impedance decreased slowly due to an increase in the silicon rubber volume at a constant volume fraction of piezoceramic. Of note, at the filling fraction values close to 0.1, the effect of V_{SR} changes is relatively enormous, and as the volume fraction approaches 0.6, the number of changes in the characteristic impedance decreases. Then, as the filling fraction reaches the value close to 0.9, the amount of the characteristic impedance reduction would increase with an increases in the V_{SR}.

Figure 11 also shows the acoustic characteristic impedance variation for 1-3 piezocomposite with three-layer polymer based on single crystal PMN-0.33PT.

As observed in Figure 11, the acoustic characteristic impedance decreases almost linearly with a decrease in the filling fraction values. In addition, as a result of increasing V_{SR} at the constant filling fraction, the value of the characteristic impedance would slowly decrease. At the filling fraction values close to 0.9 and 0.1, such decrease is considerable.

The characteristic impedance of 1-3 piezocomposite with three-layer polymer based on PMN-0.33PT at the filling fraction of approximately 0.9 is lower than that of 1-3 piezocomposite with three-layer polymer based on PZT-4 and PZT-8, indicating the better performance of PMN-0.33PT than that of the others. For a better understanding of the difference in the characteristic acoustic impedance of 1-3 piezocomposite with a three-layer polymer based on PZT-8 and PZT-4 piezoceramics and PMN-0.33PT single crystal, Figure 12 makes a comparison of the characteristic impedance of these piezocomposites at V_{SR} =50 %. Apparently, in this figure, PMN-0.33PT single crystal outperforms the other two piezoceramics PZT-8 and PZT-4 in the three-layer 1-3 piezocomposite structure.

It should be noted that the three-layer polymer in 1-3 piezocomposite can significantly improve the characteristic impedance in practice. As previously

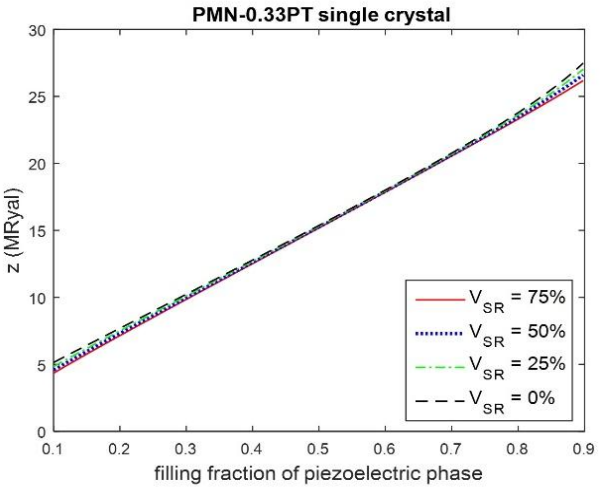

Figure 11. Variation of characteristic impedance for 1-3 piezocomposite with multi-layer polymer versus to changes in the filling fraction of piezoceramic PMN-0.33PT for different values of V_{SR}

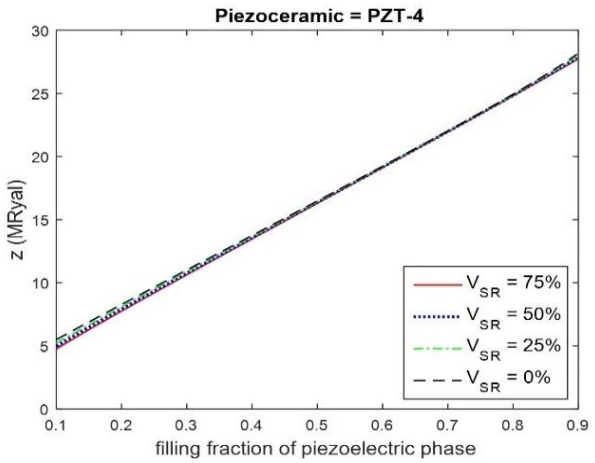

Figure 10. Variation of characteristic impedance for 1-3 piezocomposite with multi-layer polymer versus to changes in the filling fraction of piezoceramic PZT-4 for different values of V_{SR}

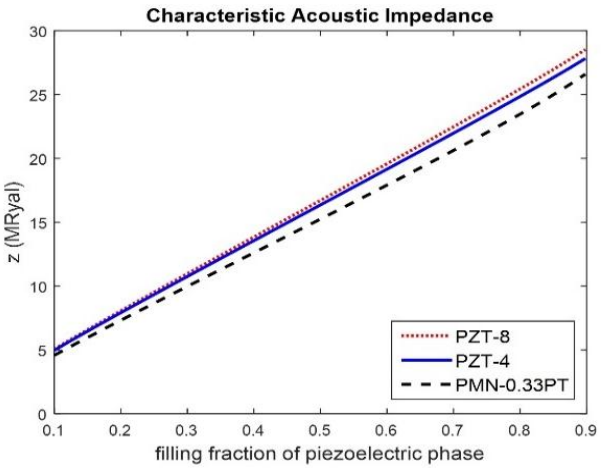

Figure 12. A comparison of the characteristic impedance of 1-3 piezocomposite with a three-layer polymer based on PZT-8 and PZT-4 piezoceramics and PMN-0.33PT single crystal at V_{SR} = 50 %

mentioned in the electromechanical coupling coefficient discussion, an increase in the V_{SR} value from 0 % to 75 % would increase the bandwidth of the filling fraction with a constant k_t value (in this filling fraction bandwidth, k_t is almost constant close to its maximum value).

This finding helps us obtain the maximum value of k_t at lower filling fractions. In other words, by reducing the filling fraction, we can obtain the highest value of k_t in lower characteristic acoustic impedances.

Next, to confirm the results obtained from the analytical method through the finite element numerical method for 1-3 piezocomposite with three-layer polymer based on piezoceramics PZT-4, PZT-8 and PMN-0.33PT single crystal at V_{SR} = 50 %, the electromechanical coupling coefficient and characteristic acoustic impedance at the filling fraction values of 0.01, 0.1, 0.2, 0.3, 0.4, 0.5, 0.6, 0.7, and 0.8 were calculated. Then, the results were compared with the graphs illustrated based on the analytical method.

Table 3 presents the results of 1-3 piezocomposite with a three-layer polymer based on PMN-0.33PT. Figure 13 shows the values for the electromechanical coupling coefficient through both analytical and numerical methods. As observed, the results obtained from the two methods agree with each other with a very good approximation.

Figure 14 represents the characteristic impedance values for 1-3 piezocomposite with three-layer polymer obtained from two analytical and numerical methods based on PMN-0.33PT single crystal at V_{SR} = 50 % for volume fractions of 0.01, 0.1, 0.2, 0.3, 0.4, 0.5, 0.6, 0.7, and 0.8. As observed, these results are also in good agreement with each other.

Next, the same operation was repeated on 1-3 piezocomposite with a three-layer polymer based on PZT-8 and PZT-4 piezoceramics. Tables 4 and 5 elaborate the results for 1-3 piezocomposite with a three-layer polymer based on PZT-8 and PZT-4. Figures 15 and 16 show the electromechanical coupling coefficient through the analytical and numerical methods.

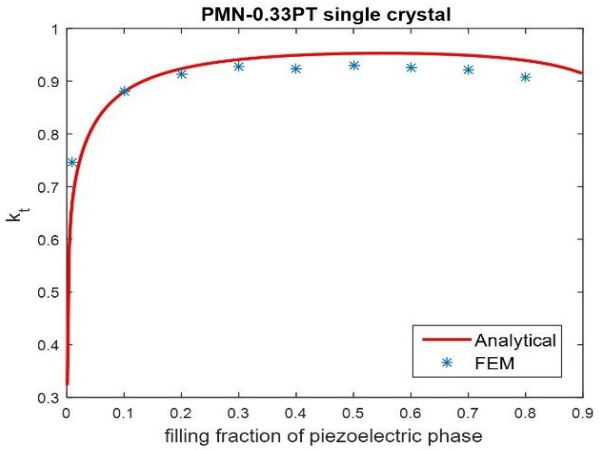

Figure 13. The electromechanical coupling coefficient obtained from two analytical and numerical methods for 1-3 piezocomposite with three-layer polymer based on PMN-0.33PT at V_{SR} = 50 %

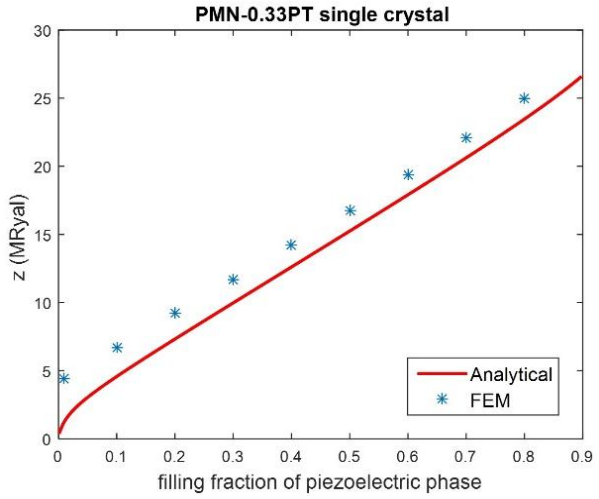

Figure 14. The characteristic impedance values obtained from two analytical and numerical methods for 1-3 piezocomposite with three-layer polymer based on PMN-0.33PT at V_{SR} = 50 %

TABLE 3. Numerical results for 1-3 piezocomposite with a three-layer polymer based on PMN-0.33PT

Filling Fraction	f_p (Hz)	f_s (Hz)	k_t	Z (Rayl)
0.8	374000	170000	0.907743	24957020
0.7	370000	156000	0.921592	22124150
0.6	367300	150400	0.926357	19415478
0.5	365000	147000	0.928922	16762625
0.4	363700	151300	0.923819	14180663
0.3	364600	148600	0.927088	11687253
0.2	366500	161200	0.914103	9206480
0.1	370000	189000	0.880671	6728450
0.01	403000	283000	0.746441	4374364

TABLE 4. Numerical results for 1-3 piezocomposite with a three-layer polymer based on PZT-8

Filling Fraction	f_p (Hz)	f_s (Hz)	k_t	Z (Rayl)
0.8	419000	342000	0.617043632	26334150
0.7	421000	341000	0.62567158	23691775
0.6	419000	337000	0.633319626	20824300
0.5	417000	337000	0.628145088	17983125
0.4	415000	335000	0.6293927	15168250
0.3	414000	335000	0.626756067	12409650
0.2	413000	337000	0.617390806	9664200
0.1	410000	341000	0.594675678	6898250
0.01	420000	393000	0.385912266	4581150

TABLE 5. Numerical results for 1-3 piezocomposite with a three-layer polymer based on PZT-4

Filling Fraction	f_p (Hz)	f_s (Hz)	k_t	Z (Rayl)
0.8	410000	324000	0.651509719	25440500
0.7	411000	324000	0.653921791	22841325
0.6	409000	319000	0.664217888	20081900
0.5	403000	318350	0.651879111	17177875
0.4	406000	318000	0.660197414	14676900
0.3	405000	318000	0.65781786	12018375
0.2	405000	321000	0.648538844	9396000
0.1	403000	328100	0.619945805	6740175
0.01	417000	380000	0.448114453	4647465

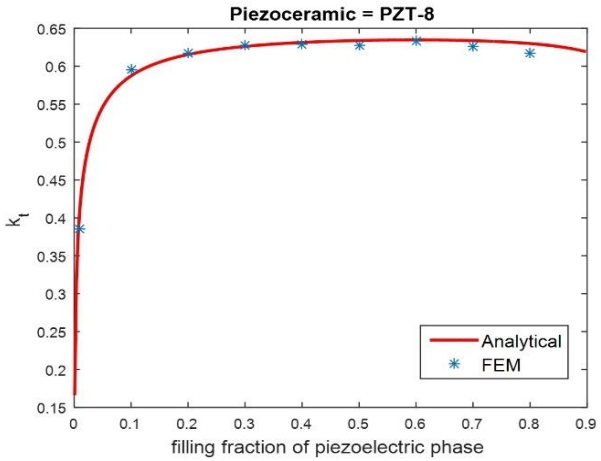

Figure 15. The electromechanical coupling coefficient obtained from two analytical and numerical methods for 1-3 piezocomposite with three-layer polymer based on PZT-8 at V_{SR} = 50 %

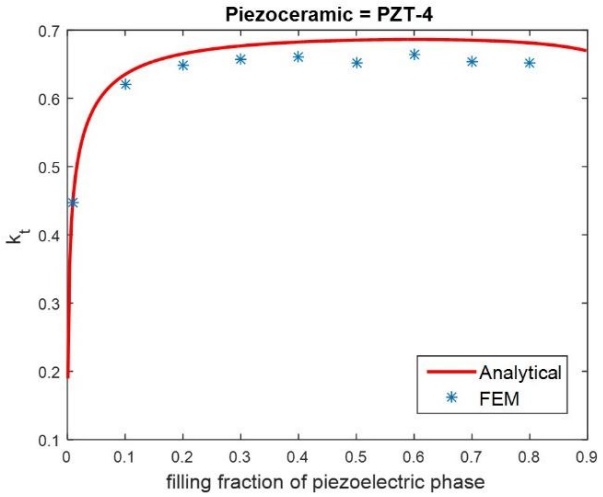

Figure 16. The electromechanical coupling coefficient obtained from two analytical and numerical methods for 1-3 piezocomposite with three-layer polymer based on PZT-4 at V_{SR} = 50 %

As observed in both piezocomposites, the results were consistent with each other for the piezocomposite based on PZT-4 and PZT-8.

Figures 17 and 18 also list the values for characteristic acoustic impedance through the numerical and analytical methods, respectively, for piezocomposite based on PZT-8 and PZT-4. In this case, the obtained results also agreed with each other.

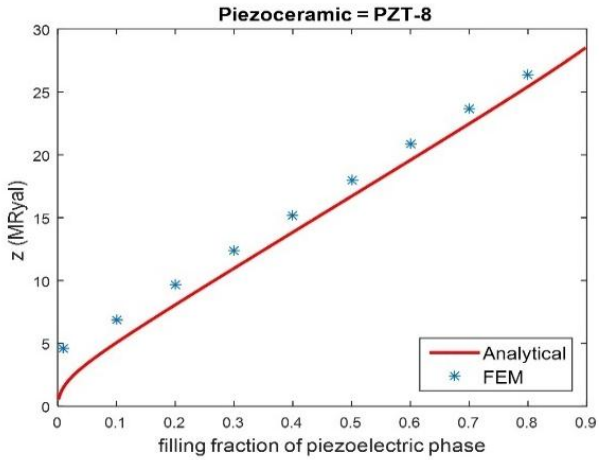

Figure 17. The characteristic impedance values obtained from two analytical and numerical methods for 1-3 piezocomposite with three-layer polymer based on PZT-8 at V_{SR} = 50%

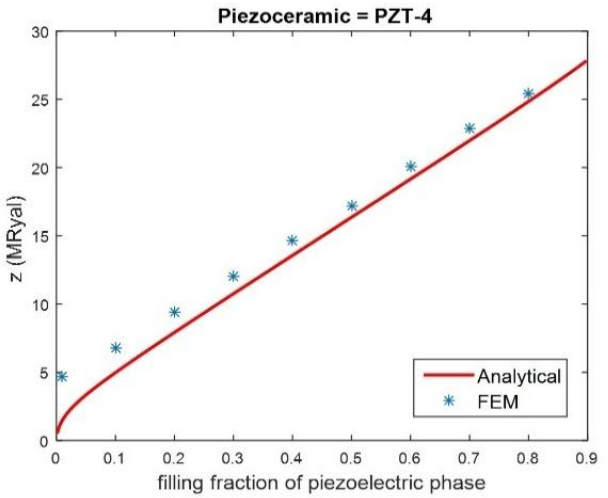

Figure 18. The characteristic impedance values obtained from two analytical and numerical methods for 1-3 piezocomposite with three-layer polymer based on PZT-4 at V_{SR} = 50 %

4. CONCLUSION

The current research aimed to produce 1-3 piezocomposite with a three-layer polymer, in which the polymer played the role of the inactive phase, and the

piezoceramic rods the role of the active phase. To obtain the parameters of the effective materials, a series of assumptions based on uniform field theories and rule of mixtures as well as the proposed relations were used to obtain the values of the electromechanical coupling coefficient, longitudinal velocity, and characteristic impedance, in terms of the coefficients of the components of the piezocomposite. In this study, 1-3 piezocomposite with a three-layer polymer was used where the middle layer is polyethylene while the other two layers are a polymer like silicone rubber, characterized by a lower stiffness coefficient (c_{11}) than that of polyethylene. Upon increasing the volume of silicone rubber, compared to that of polyethylene, the electromechanical coupling coefficient would increase while the values for longitudinal velocity and characteristic acoustic impedance of the piezocomposite would decrease. Such an increase in the volume would in turn increased the bandwidth of the filling fraction, and k_t reached its maximum value. As a result, a freedom of action was given to determine the appropriate characteristic acoustic impedance at the maximum k_t value, thus making it possible to bring the characteristic acoustic impedance as close as possible to the environment's one by reducing the filling fraction without reducing the k_t value. However, given the very good piezoelectric properties of PMN-PT single crystals, upon using these single crystals instead of PZT piezoceramics, the coupling coefficient values in piezocomposites with multi-layer polymers increased up to more than 0.95 mainly due to the higher value of the k_t coefficient and their lower stiffness coefficient (c_{11}) than those of PZT piezoceramic materials. These single crystals, due to their low stiffness coefficient (c_{11}), are characterized by much lower longitudinal velocity and characteristic impedance than those of the piezoceramics. In addition, it was observed that the degree of improvement in the piezocomposite functional parameters, including electromechanical coupling coefficient, longitudinal velocity, and characteristic impedance, was greater at low and high filling fractions (less than 0.4 and more than 0.7) than usual, indicating that implementation of this structure can be a suitable solution to improving the performance of 1-3 piezocomposite at the filling fraction values of less than 0.4 and more than 0.7. To confirm the analytical results, the values obtained from the theoretical method and finite element numerical method were compared with each other, and it was found that they were in good agreement.

ACKNOWLEDGEMENTS

The authors wish to acknowledge Payame Noor University for the all support throughout this work.

NOMENCLATURE

T	Mechanical stress tensor
S	Electric charge vector
D	Electric charge vector
E	Electric field vector
c^D	Elastic stiffness tensor in constant electrical displacement
h	Piezoelectric coefficient
β^S	Constant strain incompressibility tensor
k_t	Electromechanical coupling coefficient
ρ	Density
Z	Characteristic acoustic impedance

REFERENCES

1. Mishra, A. K., Priya, V. J. K., Pradeep, K., Vaishnav, J. S., Kabhilesh, G., "Smart materials for ultrasonic piezoelectric composite transducer: A short review", ***Materials Today: Proceedings***, Vol. 62, No. 4, (2022), 2064–2069. https://doi.org/10.1016/j.matpr.2022.02.514
2. Kamel, N. A., "Bio-piezoelectricity: fundamentals and applications in tissue engineering and regenerative medicine", ***Biophysical Reviews***, Vol. 14, No. 3, (2022), 717–733. https://doi.org/10.1007/s12551-022-00969-z
3. Cheng, L. C., Brahma, S., Huang, J. L., , Liu, C. P., "Enhanced piezoelectric coefficient and the piezoelectric nanogenerator output performance in Y-doped ZnO thin films", ***Materials Science in Semiconductor Processing***, Vol. 146, (2022), 106703. https://doi.org/10.1016/j.mssp.2022.106703
4. Akhtar, M., Raza, S., and Hasan, S., "Green Energy Harvesting from Speed Breakers using Piezoelectric Materials", ***International Journal of Research in Engineering and Science (IJRES)***, Vol. 9, No. 2, (2021), 11–16. https://ijres.org/papers/Volume-9/Issue-2/C09021116.pdf
5. Pradeesh, E. L., Udhayakumar, S., Vasundhara, M. G., Kalavathi, G. K., "A review on piezoelectric energy harvesting", ***Microsystem Technologies***, Vol. 28, No. 8, (2022), 1797–1830. https://doi.org/10.1007/s00542-022-05334-4
6. Mha, P. T., Maréchal, P., Ntamack, G. E., d'Ouazzane, S. C., "Homogenized electromechanical coefficients and effective parameters of 1–3 piezocomposites for ultrasound imaging transducers", ***Physics Letters A***, Vol. 408, (2021), 127492. https://doi.org/10.1016/j.physleta.2021.127492
7. Uchino, K., "9 - Piezoelectric composite materials", In ***Advanced Piezoelectric Materials: Science and Technology***, Woodhead Publishing, Cambridge, UK, (2010), 318–346. https://doi.org/10.1533/9781845699758.1.318
8. Li, X., Tian, J., Yan, D., Tao, C., Zhou, J., Su, Y., "Soft Mold Process for 1-3 Piezocomposite and Its Application in High Frequency Medical Ultrasound Imaging", In ***2021 IEEE International Ultrasonics Symposium (IUS)***, IEEE, (2021), 1–4. https://doi.org/10.1109/IUS52206.2021.9593444
9. Chen, D., Hou, C., Fei, C., Li, D., Lin, P., Chen, J., Yang, Y., "An optimization design strategy of 1–3 piezocomposite ultrasonic transducer for imaging applications", ***Materials Today Communications***, Vol. 24, (2020), 100991. https://doi.org/10.1016/j.mtcomm.2020.100991
10. Tian, J., Li, X., Liang, Z., Ding, W., Li, X., Tao, C., Nie, S., "Fabrication of 1–3 piezoelectric composites via modified soft mold process for 40 MHz ultrasonic medical transducers", ***Ceramics International***, Vol. 48, No. 3, (2022), 3841–3848. https://doi.org/10.1016/j.ceramint.2021.10.168
11. Lin, P., Zhu, Y., Chen, Z., Fei, C., Chen, D., Zhang, S., Li, D., Feng, W., Yang, Y., Chai, C., "Design and fabrication of non-periodic 1–3 composite structure for ultrasonic transducer application", ***Composite Structures***, Vol. 285, (2022), 115249.

https://doi.org/10.1016/j.compstruct.2022.115249

12. Wang, J., Zhong, C., Hao, S., Wang, L., "Design and Properties Analysis of Novel Modified 1-3 Piezoelectric Composite", ***Materials***, Vol. 14, No. 7, (2021). https://doi.org/10.3390/ma14071749
13. Zhong, C., Xu, J., Hao, S., Zhang, Y., Wang, L., Qin, L. "High-frequency wide beam underwater transducer based on 1–3 piezocomposite", ***Ferroelectrics Letters Section***, Vol. 48, No. 4–6, (2021), 93-103. https://doi.org/10.1080/07315171.2021.1971009
14. Wu, Q., Chen, Q., Lian, G., Wang, X., Song, X., Zhang, X., "Investigation of an air-coupled transducer with a closed-cell material matching strategy and an optimization design considering the electrical input impedance", ***Ultrasonics***, Vol. 115, (2021), 106477. https://doi.org/10.1016/j.ultras.2021.106477
15. Li, Z., Lv, J., Zhu, X., Cui, Y., Jian, X., "Development of high frequency piezocomposite with hexagonal pillars via cold ablation process", ***Ultrasonics***, Vol. 114, (2021), 106404. https://doi.org/10.1016/j.ultras.2021.106404
16. Li, F., Chen, C., Li, W., Zeng, D.,"The electro-acoustic output behavior and thermal stability of 1–3 piezoelectric composite transducers applied to FUS surgery", ***Journal of Materials Science: Materials in Electronics***, Vol. 31, No. 15, (2020), 12066–12073. https://doi.org/10.1007/s10854-020-03735-7
17. Kim, T., Cui, Z., Chang, W. Y., Kim, H., Zhu, Y., Jiang, X., "Flexible 1–3 Composite Ultrasound Transducers with Silver-Nanowire-Based Stretchable Electrodes", In ***IEEE Transactions on Industrial Electronics***, Vol. 67, No. 8, (2020), 6955-6962. https://doi.org/10.1109/TIE.2019.2937063
18. Lv, J., Xie, X., Zhu, X., Li, Z., Han, Z., Cui, Y., Zhang, B., Jian, X., "Cold ablated high frequency PMN-PT/Epoxy 1-3 composite transducer", ***Applied Acoustics***, Vol. 188, (2022), 108540. https://doi.org/10.1016/j.apacoust.2021.108540
19. Kasaeipoor Naeini, P., Delshad Chermahin, M., Shayegh Boroujeny, B., Ebadzadeh, T., Nilforoushan, M., Abdollahi, M., "Study of Dielectric Properties of Lead-Free Multiferroic KNN/22.5 $BaFe_{12}O_{19}$ Composites", ***Advanced Ceramics Progress***, Vol. 7, No. 3, (2021), 23–28. https://doi.org/10.30501/acp.2021.298611.1071
20. Xu, J., Wang, L., Zhong, C., "The effect of thickness on properties of three-phase piezocomposites", In ***IOP Conference Series: Earth and Environmental Science***, Vol. 446, No. 2, (2020), 022008. https://doi.org/10.1088/1755-1315/446/2/022008
21. Zhong, C., Wang, L., Qin, L., Zhang, Y., "Characterization of an Improved 1-3 Piezoelectric Composite by Simulation and Experiment", ***Journal of Applied Biomaterials & Functional Materials***, Vol. 15 (1_suppl), (2017), 38-44. https://doi.org/10.5301/jabfm.500036
22. Jae Lee, H., Zhang, S., Meyer Jr, R. J., Sherlock, N. P., Shrout, T. R., "Characterization of piezoelectric ceramics and 1-3 composites for high power transducers", ***Applied Physics Letters***, Vol. 101, No. 3, (2012), 032902. https://doi.org/10.1063/1.4737651
23. Cheng, K. C., Chan, H. L. W., Choy, C. L., Yin, Q., Luo, H., Yin, Z., "Single crystal PMN-0.33PT/epoxy 1-3 composites for ultrasonic transducer applications", In ***IEEE Transactions on Ultrasonics Ferroelectrics and Frequency Control***, Vol. 50, No. 9, (2003), 1177-1183. https://doi.org/10.1109/TUFFC.2003.1235328
24. Zhang, H., Wei, Z., Fan, L., Qu, J., Zhang, S., "Tunable sound transmission at an impedance-mismatched fluidic interface assisted by a composite waveguide", ***Scientific Reports***, Vol. 6, No. 1, (2016), 34688. https://doi.org/10.1038/srep34688
25. Singh, S. K., Panda, S. K., "A comparative study of micromechanics models to evaluate effective coefficients of 1-3 piezoelectric composite", ***Mechanics of Advanced Materials and Structures***, (2022), 1–14. https://doi.org/10.1080/15376494.2022.2092799
26. Sakthivel, M., Arockiarajan, A., "An analytical model for predicting thermo-electro-mechanical response of 1–3 piezoelectric composites", ***Computational Materials Science***, Vol. 48, No. 4, (2010), 759–767. https://doi.org/10.1016/j.commatsci.2010.03.027
27. Prasath, S. S., Arockiarajan, A., "Effective electromechanical response of macro-fiber composite (MFC): Analytical and numerical models", ***International Journal of Mechanical Sciences***, Vol. 77, (2013), 98–106. https://doi.org/10.1016/j.ijmecsci.2013.09.031
28. Wilson, O. B., ***Introduction to the Theory and Design of Sonar Transducers***, Peninsula Pub, (1989).
29. Yang, J., ***Mechanics of Piezoelectric Structures***, 2nd Ed., WSPC, (2020). https://doi.org/10.1142/6057
30. Balé, A., Rouffaud, R., Levassort, F., Brenner, R., Hladky-Hennion, A. C., "Homogenization of periodic 1-3 piezocomposite using wave propagation: Toward an experimental method", ***The Journal of the Acoustical Society of America***, Vol. 149, No. 5, (2021), 3122–3132. https://doi.org/10.1121/10.0004824
31. Li, L., Li-Kun, W., Lei, Q., Yuan-Yuan, W., Hong-Liang, D., Bai-Sheng, S., "The Theoretical Model for 1-3-2 Piezoelectric Composites", ***Ferroelectrics***, Vol. 350, No. 1, (2007), 29–37. https://doi.org/10.1080/00150190701369727
32. Smith, W. A., Auld, B. A., "Modeling 1-3 composite piezoelectrics: thickness-mode oscillations", In ***IEEE Transactions on Ultrasonics, Ferroelectrics, and Frequency Control***, Vol. 38, No. 1, (1991), 40–47. https://doi.org/10.1109/58.67833
33. Smith, W. A., "Modeling 1-3 composite piezoelectrics: hydrostatic response", In ***IEEE Transactions on Ultrasonics, Ferroelectrics, and Frequency Control***, Vol. 40, No. 1, (1993), 41–49. https://doi.org/10.1109/58.184997
34. Lin, P., Zhang, L., Fei, C., Li, D., Wu, R., Chen, Q., Hou, C., Yang, Y., "Novel multi-layer-composites design for ultrasonic transducer applications", ***Composite Structures***, Vol. 245, (2020), 112364. https://doi.org/10.1016/j.compstruct.2020.112364